phys. stat. sol. (b) **245**, No. 10, 2111–2114 (2008) / **DOI** 10.1002/pssb.200879656

physica status solidi b
www.pss-b.com
basic solid state physics

Effects of a ZnS-shell on the structural and electronic properties of CdSe-nanorods

M. Mohr* **and C. Thomsen**

Institut für Festkörperphysik, Technische Universität Berlin, Hardenbergstr. 36, 10623 Berlin, Germany

Received 6 June 2008, revised 16 July 2008, accepted 18 July 2008
Published online 3 September 2008

PACS 61.46.-w, 61.72.uj, 63.22.Gh, 74.25.Jb

* Corresponding author: e-mail marcel@physik.tu-berlin.de

CdSe nanorods were studied via density functional theory calculations. The influence of a ZnS shell on the structural and electronic properties was investigated. The ZnS shell leads to a shortening of the CdSe bond length, the magnitude depending on the bond length orientation with respect to the axis. The electronic band gap is reduced by the presence of the ZnS shell. In the present study, the CdSe/ZnS multistructure forms a type II heterojunction, in contrast to plane CdSe/ZnS superlattices.

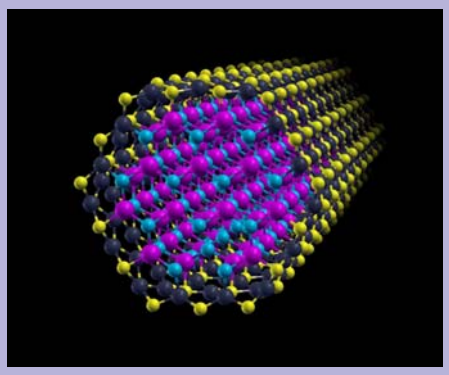

Atomic structure of a CdSe nanorod with a surrounding ZnS shell.

1 Introduction CdSe nanostructures have become an important field in solid state physics, especially due to the recent advances in the growth synthesis. The fabrication of colloidal CdSe nanocrystals allows the growth of nanorods with defined aspect ratios and sizes [1–3]. CdSe nanorods have promising optical properties for applications in low-threshold lasers or solar harvesting cells [4]. Growing a graded CdS/ZnS shell on the CdSe rods improves the quantum efficiency and decreases the laser threshold [5,6]. However, details about the shell and its influence on the CdSe core are difficult to obtain due to the lack of sufficient TEM resolution and the small X-ray structure factor of ZnS compared to CdSe. While there has been considerable effort in understanding the structural and electronic properties of CdSe nanorods from theory [3,7] there have been little efforts to understand the effects of a surrounding ZnS shell.

In the present work we exploit *ab-initio* calculations for a structural analysis of the core-shell composition. Analyzing the structural properties of a CdSe nanorod with a ZnS shell we demonstrate that bonds are shortened differently depending on their orientation to the axis. We further demonstrate, that the CdSe/ZnS nanorod transforms from a type-I into a type-II heterojunction.

2 Calculation The nanorods were created on the basis of wurtzite-structured nanocrystals with a cylindrical shape. They were regarded as infinite along their growth direction, *i.e.*, the c-axis. The cross section of the relaxed nanorods is shown in Fig. 1a. To investigate the influence of a ZnS shell, we performed calculations on a nanorod and a nanorod with a ZnS shell (rod I and III). To compare the effects of the ZnS shell with size dependent effects, we also calculate a nanorod without a shell of the same size (rod II). The total number of atoms in the unit cell were 48 and 108 for rod I and II/III, respectively. The ZnS shell consisted of 60 atoms. We employ the local density approximation [8] of the density functional theory with

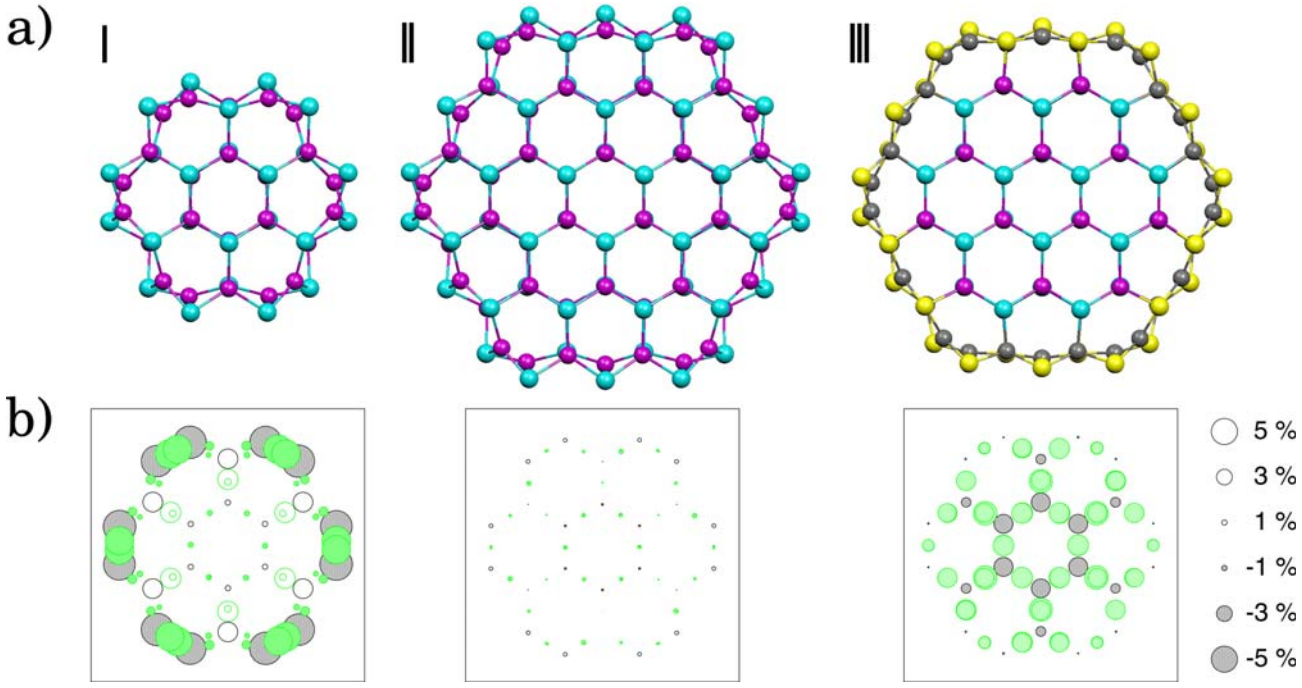

Figure 1 Cross sections of the CdSe nanorods (upper row) and bond length deviations compared to bulk CdSe (lower row).

atom-centered confined numerical basis functions as implemented in the SIESTA code [9, 10]. Norm-conserving pseudopotentials were generated with the Troullier Martins scheme [11] for the following valence-state configurations: Se $4s^2$ (1.89) $4p^4$ (1.89), Cd $5s^2$ (2.18) $4d^{10}$ (2.5), Zn $4s^2$ (2.43) $3d^{10}$ (2.09), S $3s^2$ (1.63) $3p^4$ (1.76), where the value in parenthesis indicates the pseudopotential core radii in bohr. The valence electrons were described by a double-ζ basis set plus an additional polarizing orbital. The localization of the basis followed the standard split scheme and was controlled by an internal SIESTA parameter, the energy shift, for which a value of 50 meV was used. This resulted in basis functions with a maximal extension of 3.45 Å(Se), 4.13 Å(Cd), 3.29 Å(S) and 3.81 Å(Zn). Periodic images of the nanorods were separated by at least 20 Å. Real space integrations were performed on a grid with a fineness of 0.16 Å, which can represent plane waves up to an energy of 120 Ry. The nanowire structures were relaxed until all forces were below 0.02 eV/Å. Stress components along the wire axes were minimized with respect to the c-lattice constant. For bulk CdSe and ZnS a $(6 \times 6 \times 4)$ Monkhorst-Pack [12] mesh in reciprocal space was used, whereas a minimum of 8 k-points equally spaced along the 1D Brillouin zone was used for the nanorods. The deviations from the bulk lattice constants were found to be small (<1 %) for wurtzite CdSe and ZnS. Another test for the validity of our calculations is the bulk modulus and values of 55.5 and 80.2 GPa were obtained for CdSe and ZnS, respectively, in good agreement with the experimental values of 53.4 and 76.0 GPa [13, 14].

From the relaxed cross sections in Fig. 1a can be seen that the most dramatic changes in the atomic structure happen in the outermost monolayer: the Cd or Zn-atoms rotate into the surface to lower the energy. We also have calculated the nanorods with a passivating hydrogen shell and have not found qualitative changes of this reconstruction. This reconstruction was first reported by Ref. [15].The effect of the surface reconstruction becomes smaller after the first monolayer. The crystal structure of bulk CdSe is resembled with small deviations, as can be seen in rods I and II.

3 Results and discussion Figure 1b shows the bond lengths of the relaxed CdSe nanorods projected on the plane perpendicular to the c-axis. The bonds are centered in the middle of the atoms they connect. The radius of the circles is proportional to the deviation from the bulk CdSe bond length. Black circles correspond to bonds parallel to the c-axis, green (gray) circles correspond to all other bonds.

The ZnS shell that surrounds rod III leads to a compressive strain of the CdSe core due to the small lattice parameter of ZnS. The diameter d of rod III is ≈ 5 % smaller than that of rod II (see Table 1). Figure 1b shows that all bonds of the CdSe core are shortened. The bonds in lateral direction are more strongly compressed than the bonds parallel to the c-axis. For the lateral bonds the average decrease is 3.5 %, while it is 1.5 % for the bonds parallel to c. The maximal decrease is 4.5 % and 3.6 % for lateral and parallel bonds, respectively. The bonds parallel to the c-axis

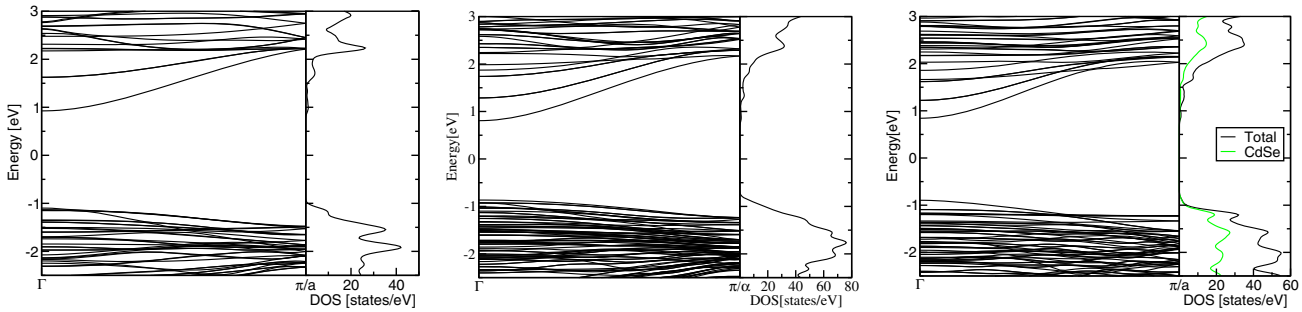

a) Rod I b) Rod II c) Rod III

Figure 2 Band structure and DOS (Gaussian broadening of 0.1 eV). In the DOS of rod III we plot the projected DOS of the CdSe atoms.

show the trend of being less compressed when lying closer to the surface. In contrast, the lateral bonds are homogeneously compressed throughout the CdSe core.

Our results show a good agreement with experiments on CdSe/ZnSe nanocrystals. ZnSe has nearly half the lattice mismatch than ZnS, therefore the observed decrease in the experiment is expected to be smaller than in our calculations. The authors of Ref. [16] find a decrease of 1.234 % and 1.511 % for the parameters a and c. The nanocrystals they investigate are spherical, which may explain the similar decrease for a and c, in contrast to our cylindrically shaped rods.

Table 1

	Rod I	Rod II	Rod III	Rod I (GGA)[1]
diameter d (Å)	13.7	21.7	20.5	–
calc. band gap (eV)	1.97	1.67	1.74	2.1

[1] Ref. [17]

Additionally to the changes in bond length, we investigated the changes in the electronic band structure. Bulk CdSe has a direct electronic band gap. Absorption or photoluminescence measurements revealed that the band gap of CdSe nanocrystallites show a strong size dependence [3]. Figure 2 shows the calculated band structure and the electronic density of states of the rods shown in Figure 1. As expected we find the direct band gap for the CdSe rods that is strongly size dependent. Further analysis of the size dependence and the effect of a passivating hydrogen shell is given in Ref. [18]. The inability of the LDA to precisely predict excited energies leads to an underestimation of the band gaps. This is usually corrected using the scissors operator. We have refrained from using it here, as we use two different material systems. For rod I the authors of Ref. [17] find a band gap 2.1 eV using GGA.This is close to our LDA value of 1.97 eV.

The band gap of the core-shell rod is slightly lower than that of the pure rod. The calculated values are summarized in Table 1. The number of states in the minimum of the conduction band is small in all rods. For the rod III we plot the DOS projected on the CdSe atoms, to better visualize the effect of the ZnS-shell. This PDOS suggest that the lowest band stems from the ZnS shell. This, however, influences the type of junction that is formed by the multistructure. If the band-gap of the core is enclosed by that of the shell material, this configuration is known as type I, and the electron and hole wave functions may be confined in the core region. The classification is done *via* an analysis of the bulk band structure and the bulk workfunction of the corresponding materials. The band diagram we obtain within our calculations of bulk material is shown in Fig. 3a. This is in agreement with other work that classify CdSe/ZnS heterojunction as type I [19]. A detailed analysis of the valence band maximum (VBM) and the conduction band minimum (CBM) shows that for small systems like here, the CdSe/ZnS junction turns into a type II system, where the band gaps are staggered. The squares of the wavefunction of the CBM and the VBM were added for 8 equidistant planes within the unit cell and plotted in Figs. 3b and c. The valence band maximum is strictly confined to the core region. The conduction band minimum is strongly located on the ZnS shell. This may have important consequences for applications. Core shell nanowires have been recently discovered to serve as solar cells [20]. An advantage of this core/shell architecture is that carrier separation takes place in the radial direction whereas carrier transport is done along the axial direction. And as electrons are confined in the core and the holes are confined in the shell recombination is minimized. This has been predicted for GaN-GaP nanowires [21]. We expect that, if the core or shell become larger, the CdSe/ZnS system becomes a type I system again.

4 Summary Summarizing, we have presented results on *ab initio* calculations of CdSe and CdSe/ZnS core/shell nanorods. By comparing the results with and without a shell, we analyze the effect of the shell on the structural and electronic properties. The bond lengths of the CdSe core are reduced differently depending on the orientation of the bond to the axis. Due to the small system size, the CdSe/ZnS heterostructure, usually characterized as type-I

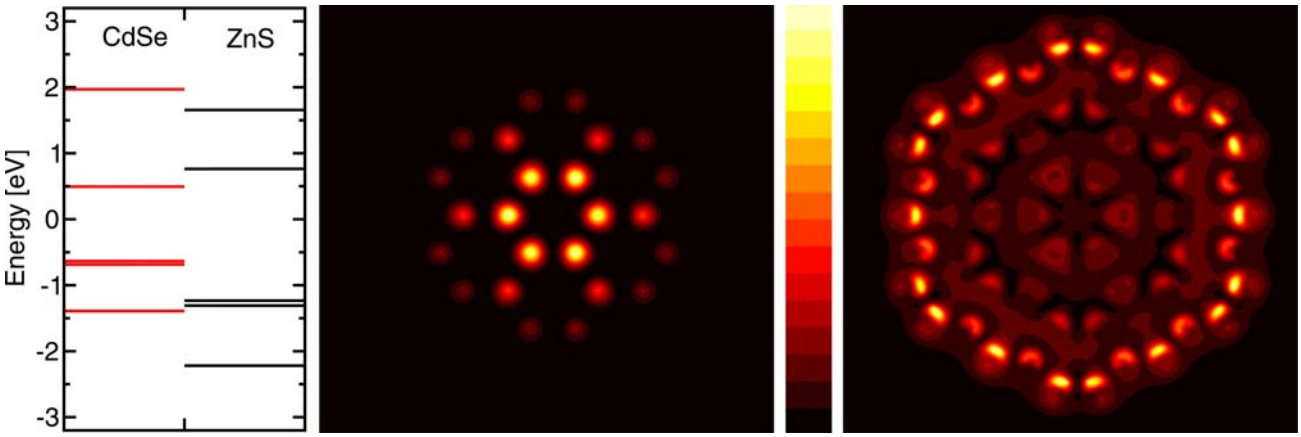

Figure 3 Cross-section views of the charge distribution of the CBM electron state and VBM hole state in core-shell nanorods. The atomic structure is that of rod III in Fig. 1.

junction turns into a type-II junction, opening possibilies for new applications of CdSe/ZnS core/shell nanorods.

References

[1] X. Peng, L. Manna, W. Yang, J. Wickham, E. Scher, A. Kadavanich, and A. P. Alivisatos, Nature **404**, 59–61 (2000).
[2] L. s. Li, J. Hu, W. Yang, and A. P. Alivisatos, Nano Lett. **1**(7), 349–351 (2001).
[3] H. Yu, J. B. Li, R. A. Loomis, P. C. Gibbons, L. W. Wang, and W. E. Buhro, J. Amer. Chem. Soc. **125**, 16168 (2003).
[4] W. U. Huynh, J. J. Dittmer, and A. P. Alivisatos, Science **295**(5564), 2425–2427 (2002).
[5] L. Manna, E. C. Scher, L. S. Li, and A. P. Alivisatos, J. Am. Chem. Soc. **124**(24), 7136–7145 (2002).
[6] M. Kazes, D. Y. Lewis, Y. Ebenstein, T. Mokari, and U. Banin, Adv. Mater. **14**, 317–321 (2002).
[7] T. Sadowski and R. Ramprasad, Phys. Rev. B **76**, 235310 (2007).
[8] J. P. Perdew and A. Zunger, Phys. Rev. B **23**, 5048 (1981).
[9] P. Ordejón, E. Artacho, and J. M. Soler, Phys. Rev. B **53**, R10 441 (1996).
[10] J. M. Soler, E. Artacho, J. D. Gale, A. García, J. Junquera, P. Ordejón, and D. Sánchez-Portal, J. Phys.: Condens. Matter **14**, 2745 (2002).
[11] N. Troullier and J. L. Martins, Phys. Rev. B **43**, 1993 (1991).
[12] H. J. Monkhorst and J. D. Pack, Phys. Rev. B **13**, 5188 (1976).
[13] B. Bonello and B. Fernandez, J. Phys. Chem. Solids **54**(2), 209–212 (1993).
[14] E. Chang and G. R. Barsch, J. Phys. Chem. Solids **34**(9), 1543–1563 (1973).
[15] D. M. Aruguete, M. A. Marcus, L. S. Li, A. Williamson, S. Fakra, F. Gygi, G. A. Galli, and A. P. Alivisatos, J. Phys. Chem. C **111**, 75–79 (2007).
[16] Y. J. Lee, T. G. Kim, and Y. M. Sung, Nanotechnology **17**, 3539 (2006).
[17] S. P. Huang, W. D. Cheng, D. S. Wu, J. M. Hu, J. Shen, Z. Xie, H. Zhang, and Y. J. Gong, Appl. Phys. Lett. **90**, 031904 (2007).
[18] M. Mohr and C. Thomsen (submitted, preprint arXiv:0802.3975v2).
[19] H. Mattoussi, L. H. Radzilowski, B. O. Dabbousi, E. L. Thomas, M. G. Bawendi, and M. F. Rubner, J. Appl. Phys. **83**(12), 7965–7974 (1998).
[20] B. Tian, X. Zheng, T. J. Kempa, Y. Fang, N. Yu, G. Yu, J. Huang, and C. M. Lieber, Nature **449**, 885–889 (2007).
[21] Z. Y. Zhang, W. L. Wang, and M. A. Mascarenhas, Nano Lett. **7**(5), 1264–1269 (2007).

